*At*RabF2b (Ara7) acts on the vacuolar trafficking pathway in tobacco leaf epidermal cells

Amanda M. Kotzer[1], Federica Brandizzi[2], Ulla Neumann[1], Nadine Paris[3], Ian Moore[4] and Chris Hawes[1,*]

[1]Research School of Biological and Molecular Sciences, Oxford Brookes University, Gipsy Lane, Oxford, OX3 0BP, UK
[2]Department of Biology, University of Saskatchewan, S7N 5E2, Canada
[3]UMR-CNRS 6037, Université de Rouen, 76821 Mont Saint Aignan, France
[4]Department of Plant Sciences, University of Oxford, South Parks Road, OX1 3RB, UK
*Author for correspondence (e-mail: chawes@brookes.ac.uk)

Accepted 24 September 2004
Journal of Cell Science 117, 6377-6389 Published by The Company of Biologists 2004
doi:10.1242/jcs.01564

Summary

Rab GTPases are universal key regulators of intracellular secretory trafficking events. In particular, Rab 5 homologues have been implicated in endocytic events and in the vacuolar pathway. In this study, we investigate the location and function of a member of this family, *At*RabF2b (Ara7) in tobacco (*Nicotiana tabacum*) leaf epidermal cells using a live cell imaging approach. Fluorescent-tagged *At*RabF2b[wt] localized to the prevacuolar compartment and Golgi apparatus, as determined by coexpression studies with fluorescent markers for these compartments. Mutations that impair *At*RabF2b function also alter the subcellular location of the GTPase. In addition, coexpression studies of the protein with the vacuole-targeted aleurain-green fluorescent protein (GFP) and rescue experiments with wild-type *At*RabF2b indicate that the dominant-negative mutant of *At*RabF2b causes the vacuolar marker to be secreted to the apoplast. Our results indicate a clear role of *At*RabF2b in the vacuolar trafficking pathway.

Supplementary material available online at
http://jcs.biologists.org/cgi/content/full/117/26/6377/DC1

Key words: Rab GTPase, Prevacuolar compartment, Golgi apparatus, Plant secretory pathway

Introduction

The endoplasmic reticulum (ER), the Golgi apparatus, the vacuole and the plasma membrane constitute the major components of the plant secretory system. The communication between these organelles is mediated by small GTPases of the Rab subfamily (Stenmark and Olkkonen, 2001). Members of this family are localized to distinct membrane compartments and exert functions in different trafficking steps in the secretory and endocytic pathways. Specifically, Rab proteins are involved in the recruitment of effector molecules on cellular membranes, which in turn regulate membrane docking and fusion (Stenmark and Olkkonen, 2001).

Rab GTPases are soluble proteins of ~23 kDa and contain conserved amino acid sequences, which are necessary for nucleotide binding and GTP hydrolysis (Olkkonen and Stenmark, 1997). They act as molecular switches that regulate intracellular transport cycling between a target membrane and the cytosol, by alternating between GTP and GDP conformations (Bourne et al., 1991; Nuoffer and Balch, 1994; Scheffzek et al., 1998; Wittinghofer, 1998; Zerial and McBride, 2001).

In *Arabidopsis* there are 57 members of the Rab GTPase family. In phylograms, all plant Rab sequences can be grouped into just eight clades, named A to H (Rutherford and Moore, 2002). These clades are related to the six Rab subclasses that are common to yeasts and animals. The RabF branch contains three sequences divided into two putative subclasses RabF1 and RabF2. Three homologues identified in *Arabidopsis*, *At*RabF1 (Ara6), *At*RabF2a (Rha1) and *At*RabF2b (Ara7) are similar to Rab5 and Rab22 of mammals and to Ypt51/Ypt52/Ypt53 in yeast, which are involved in the endocytic and vacuolar trafficking pathway (Bucci et al., 1992; Olkkonen et al., 1993; Singer-Kruger et al., 1994).

The role of the plant Rab5 homologues is presently not clearly defined. Investigations into these proteins have indicated roles in both the endocytic and vacuolar trafficking pathways. In *Arabidopsis* protoplasts, *At*RabF1 (Ara6) the unique myristoylated Rab protein of the *Arabidopsis* genome and the conventional orthologue of Rab5, *At*RabF2b (Ara7) were reported to be involved in the endocytic pathway. This suggestion was based on coexpression studies using the fluorescent internalization marker FM4-64 in protoplasts expressing *At*RabF1 or *At*RabF2b (Ueda et al., 2001). Both proteins were suggested to localize to putative endosomal structures (Ueda et al., 2001).

In *Arabidopsis* root epidermal cells, *At*RabF1-GFP was used as an endosomal marker to investigate the trafficking of filipin in the early endocytic pathway (Grebe et al., 2003). *At*RabF1 colocalized intracellularly with the filipin-sterol fluorescence and it was concluded that early endocytic sterol trafficking involves transport via *At*RabF1-positive early endosomes (Grebe et al., 2003).

*At*RabF2b has been used as a marker for endocytic studies (Geldner et al., 2003) where GFP-*At*RabF2b was transiently

expressed in cell lines in which the ARF-GEF, GNOM, was mutated. In these cells, the size and shape of the *At*RabF2b-labelled compartments were altered; evidence that was taken as an indication that *At*RabF2b is involved in the endocytic pathway in *Arabidopsis* roots (Geldner et al., 2003).

In contrast to the suggested roles of *At*RabF1 and *At*RabF2b in the endocytic pathway, the third *Arabidopsis* isoform closely related to mammalian Rab5, *At*RabF2a (Rha1) was recently suggested to play a role in the trafficking of soluble cargo from the prevacuolar compartment (PVC) to the lytic vacuole (Sohn et al., 2003). In *Arabidopsis* protoplasts, the GDP-locked dominant-negative inhibitory mutant *At*RabF2a[S24N], either tagged with the small epitope haemagglutinin (HA) or fused to red fluorescent protein (RFP), was shown to inhibit transport of GFP fused to the soluble vacuolar markers sporamin (Spo:GFP) and *Arabidopsis* aleurain-like protein (AALP:GFP) to the central vacuole. By contrast, the HA-tagged dominant-negative S47N mutant of the unique myristoylated homologue *At*RabF1 (Ara6) did not affect the distribution of SpoGFP. It was also suggested that the *At*RabF2a wild type partially relieved the inhibitory effect of RFP-*At*RabF2a[S24N]. Finally, immunolabelling of protoplasts expressing RFP-*At*RabF2a[S24N] with an antibody to the vacuolar sorting receptor (VSR) led to the conclusion that this Rab protein was localized to the PVC (Sohn et al., 2003).

Additional investigation on the RabF class was carried out on another homologue of *At*RabF1 isolated from *Mesembryanthemum crystallinum* (Bolte et al., 2000), termed m-$Rab_{mc,}$ and closely related to the *Arabidopsis* homologue RabF1 (Bolte et al., 2004a). Despite its high degree of sequence similarity to *At*RabF1, m-Rab_{mc} has been predominantly localized on the pre-vacuolar compartment of the lytic vacuole and on the Golgi apparatus. The authors showed that the dominant-negative mutant of m-Rab_{mc} inhibited the transport of aleurain GFP, a soluble vacuolar marker, in *Arabidopsis thaliana* protolasts (Bolte et al., 2004a). This contradiction on the role of these Rabs, even within the same model experimental system, raises the issue that the location and function of the plant Rab5 homologues have yet to be conclusively proved and differences, if any, between early endocytic compartments (endosomes) and prevacuolar compartments need to be clarified.

The purpose of this study was to gain further insight on the role of *At*RabF2b in the secretory pathway in plants. To do this, we coexpressed known vacuolar markers along with untagged and fluorescent chimaeras of *At*RabF2b and mutants that impair its ability to exchange activated nucleotides and binding to membranes. Our results indicate a clear role of *At*RabF2b in the vacuolar trafficking pathway in tobacco leaf epidermal cells.

Materials and Methods

Generation of mutant versions of AtRabF2b, fluorescent protein tagging and molecular cloning

Standard molecular techniques were used as described (Ausubel et al., 1999). The cDNA of wild-type *At*RabF2b, was amplified using primers AMK03 5′-GCTCCTGGATCCGGTGGTATGGCTGCAG-CTGGAAACAAGAGC-3′ and UN02 3′-CCGGCCGAGCTCCT-AAGCACAACACGATGAACTCAC-5′ adding *Bam*HI and *Sac*I restriction sites (underlined), respectively. The resulting PCR product was cloned into pVKH18-En6 (Batoko et al., 2000) with either mGFP5 or EYFP (Clontech, Palo Alto, CA) at the N-terminus of *At*RabF2b.

Mutations in functionally important regions of *At*RabF2b were created using site-directed mutagenesis. The *At*RabF2b[S24N] mutant was generated from *At*RabF2b with primers 5′-GT-TGGTGCTGGAAAAAACAGTCTTGTGTTACGG-3′ and UNO2; AMK03 and 3′-CCGTAACACAAGACTGTTTTTTCCAGCAC-CAAC-5′. *At*RabF2b[Q69L] was generated with the following primers using *At*RabF2b as a template 5′-GTGAAGTTTGAGATT-TGGGATACTGCAGGTCTCGAACGGTACCATAGTTTG-3′ and UNO2; AMK03 and 3′-CAAACTATGGTACCGTTCGAGACCT-GCAGTATCCCAAATCTCAAACTTCAC-5′. The *At*RabF2b[N123I] mutation was introduced into *At*RabF2b using 5′-GGTAACCCTA-ATATGGTCATGGCGCTAGCTGGAATCAAATCTGATTTATTAG-ATG-3′ and UNO2; AMK03 and 3′-ATCTAATAAATCAGATTTG-ATTCCAGCTAGCGCCATGACCATATTAGGGTTACC-5′.
*At*RabF2b[C198,199S] was created from *At*RabF2b using the primers AMK03 and 3′-CCGGCCGAGCTCCTAAGCAGAAGACGATGA-ACTCACTGCCCTATC-5′.

Untagged versions of *At*RabF2b and mutants were generated by PCR from the fluorescent-tagged forms, inserting *Xba*I at the 5′ region using 5′-CAGGACCTCTAGATGGCTGCAGCTGGAAACAAGA-GC-3′ (*Xba*I site underlined). The resulting PCR product was subcloned into pVKH18-En6 lacking the fluorescent tag.

Transient expression in plant

Nicotiana tabacum plants were grown in a greenhouse at 21°C with natural day length illumination. For experimental use, plants were transferred to a plant growth chamber at 21°C with a 12-hour light and 12-hour dark regime. Each construct was mobilized in *Agrobacterium tumefaciens* strain GV3101::pMP90 by freeze-thawing (Höfgen and Willmitzer, 1988) followed by selection on YEB plates containing the appropriate antibiotics. *Agrobacterium*-mediated transient expression in tobacco leaf epidermal cells was conducted as previously described (Batoko et al., 2000; Brandizzi et al., 2002a; Geelen et al., 2002). For expression of each construct alone or in combination, the level of inoculum was adjusted as specified for each experiment (see figure legends).

Fluorescent markers

The secreted GFP marker (secGFP), and the Golgi-targeted markers (ST-GFP and its spectral variant ST-YFP), have been previously described (Batoko et al., 2000; Brandizzi et al., 2002a; Brandizzi et al., 2002b). Aleurain-GFP (Humair et al., 2001) and BobTIP26-1::GFP (Reisen et al., 2003) were constructed as described.

To label the prevacuolar compartment, GFP or YFP was fused to the transmembrane and cytosolic sequence of pea BP80 (Paris et al., 1997). The construct called PS1 is identical to BP19 described (Brandizzi et al., 2002a) except that all of the cytosolic amino acids are present. BP19 contains the coding sequence of GFP6, which has two mutations F64L and S65T (Cormack et al., 1996), followed by the coding sequence of the transmembrane domain of the peaBP80 (GenBank accession number T18301) (Brandizzi et al., 2002a) and the first five amino acids of the cytosolic region of peaBP80. In BP19, the pea BP80 nucleotide sequence is flanked by a *Sal*I site at the 5′ end and by a *Sac*I site at the 3′ end. A new fragment was made by polymerase chain reaction of peaBP80 sequence to generate a *Sal*I site at amino acids 563 and 564 and a *Sac*I site at the original stop codon position. The *Sal*I-*Sac*I fragment was confirmed by sequencing and inserted into BP19 in place of the truncated version. For the YFP version of PS1, a *Sal*I site was added at the 3′ end of the YFP coding sequence at the same position as GFP and the GFP sequence from PS1 was replaced by the YFP. Finally, both GFP and YFP versions of PS1 were subcloned into the binary vector pVKH18-EN6 into the restriction sites *Xba*I and *Sac*I.

Confocal imaging and fluorescence quantification

Unless otherwise stated, infected cells of the lower epidermis of transformed leaves were analysed 48-72 hours after inoculation. Confocal imaging was performed using an upright or inverted Zeiss LSM 510 Laser Scanning Microscope (Jena, Germany) with a 40×, N.A. 1.30, oil-immersion lens. For multi-track imaging, GFP was excited with a 458 nm wavelength of an argon line; the emission was collected using a 505-530 nm band pass filter and EYFP was excited with a 514 nm wavelength of an argon line; the emission was collected using a 535-590 nm band pass filter. Fluorescence quantification was done from low magnification 12 bits images (acquired using a 10× lens) using LSM 510 software. Post-acquisition processing of images was done using the Zeiss LSM 510 software (Jena, Germany) and Adobe Photoshop 7.0 (Mountain View, CA) software.

Western blot analysis

Proteins were extracted from tobacco leaves transiently expressing fluorescent protein-tagged *At*RabF2b fusions, and gel electrophoresis and blotting was carried out as described (Batoko et al., 2000). The blot was probed with a polyclonal antibody raised against GFP (1:2000 dilution, Molecular Probes, Leiden, The Netherlands) followed by an alkaline phosphatase-conjugated secondary antibody (1:1000 dilution, DAKO, Denmark). The results were determined with the BCIP/NBT colour development substrate (Promega, UK) according to the manufacturer's recommendations.

Results

Location of *At*RabF2b chimaeras

As important regulators in membrane traffic, many Rab proteins are known to cycle on and off specific membranes in a nucleotide-dependent manner (Olkkonen and Stenmark, 1997). To investigate the location of *At*RabF2b (Ara7), green (GFP) or yellow (YFP) fluorescent protein was fused to the N-terminus of the Rab. To investigate the nucleotide dependency of *At*RabF2b, mutations were introduced in functionally important regions responsible for GTP binding and hydrolysis activities. The resulting mutants were analysed for altered location and function.

Two to three days after *Agrobacterium*-mediated transformation, the fusion protein was analysed in vivo in tobacco leaf epidermal cells by confocal microscopy. YFP-*At*RabF2b[wt] and YFP-*At*RabF2b[S24N] were expressed in punctate, mobile organelles less than 1μm in diameter and also in the cytosol, whereas GFP-*At*RabF2b[Q69L] labelled 1-2 μm spherical structures and a membrane close to the periphery of the cell (Fig. 1A-C).

To determine the nature of the GFP-*At*RabF2b[wt]-positive punctate structures, which resemble the pattern described for the plant Golgi apparatus (Boevink et al., 1998), GFP-*At*RabF2b[wt] was coexpressed with a Golgi marker, ST-YFP (Brandizzi et al., 2002a). GFP-*At*RabF2b[wt] labelled two populations of structure, one that colocalized with ST-YFP and one that did not (Fig. 1D,E). This indicates that the *At*RabF2b[wt] protein is resident on the Golgi and at least one other organelle.

Tagged *At*RabF2b[S24N] was created by substituting serine24 for asparagine, within the conserved PM1 (phosphate/magnesium-binding) motif. This protein is predicted to have a higher affinity to GDP, resulting in an inactive form of the protein (Olkkonen and Stenmark, 1997). When expressed transiently in tobacco leaf epidermal cells, GFP-*At*RabF2b[S24N] labelled punctate structures and the cytosol (Fig. 1F, green channel). The punctate structures observed completely colocalized with ST-YFP (Fig. 1F, merged image).

Tagged *At*RabF2b[Q69L] was created by changing glutamine69 to leucine. This mutation, within the conserved PM3 motif, is predicted to have lower intrinsic GTPase activity, therefore promoting the GTP-bound state (Olkkonen and Stenmark, 1997). GFP-*At*RabF2b[Q69L] labelled larger spherical structures (1-2 μm in diameter) and a membrane close to the boundaries of the cell (Fig. 1C,G). The spherical structures did not colocalize with ST-YFP, nor did ST-YFP fluorescence accumulate within the spheres (arrow, Fig. 1G). When the YFP-*At*RabF2b[Q69L] construct was coexpressed with BobTIP26-1::GFP, previously shown to label the tonoplast (Reisen et al., 2003), the fusion proteins colocalized on the same membrane (arrow, Fig.1H). When BobTIP26-1::GFP was infiltrated alone into tobacco leaf epidermal cells, as expression level increased, spheres similar to those shown in Fig. 1H green channel were observed (data not shown). These structures were not apparent in tobacco protoplasts and BY2 suspension cells singly expressing the BobTIP26-1::GFP construct (Reisen et al., 2003). Additionally, the number of spheres normally observed in cells expressing the tagged *At*RabF2b[Q69L] alone, compared to when coexpressed with BobTIP26-1::GFP, appeared to increase [compare Fig. 1C and G (green channel) to H (red channel)].

The absence of labelling of the plasma membrane by the fluorescent mutant was verified upon coexpression with a plasma membrane marker (*Nt*AQP1-XFP, a plasma membrane aquaporin; A.M.K., unpublished results), as tagged-*At*RabF2b[Q69L] did not localize with the fluorescent aquaporin (data not shown).

A nucleotide-free form of *At*RabF2b was created by mutations within the conserved guanine-base-binding motif G2, changing asparagine123 to isoleucine. This mutation reduces the affinity of the protein to both GDP and GTP (Olkkonen and Stenmark, 1997). When expressed in leaf epidermal cells, YFP-*At*RabF2b[N123I] was entirely cytosolic (Fig. 1I).

Cysteine motif isoprenylation on the variable C-terminus is essential for specific attachment of Rab GTPases to membranes and for their recognition by Rab GDP dissociation inhibitor (GDI) (Olkkonen and Stenmark, 1997). To eliminate the isoprenylation site at the C-terminus of *At*RabF2b, the cysteine residues at positions 198 and 199 were mutated to serines. The YFP-*At*RabF2b[C198, 199S] was entirely cytosolic (Fig. 1J). These results are consistent with the lack of insertion into membranes because of the absence of a functional isoprenylation motif.

Nucleotide-free Rab mutants have been shown to be unstable (Olkkonen and Stenmark, 1997). To investigate the stability of the mutated forms of *At*RabF2b and to determine whether the cytosolic labelling pattern of the *At*RabF2b[N123I] fusion resulted from loss of its RabF2b moiety, immunoblot analysis of extracts from transformed leaves was performed (Fig. 2A). Equal amounts of protein were loaded in each lane (Fig. 2B) and the amount of epitope recognized by the anti-GFP antibody in the GFP-*At*RabF2b[N123I] did not appear to be significantly lower than the GFP-*At*RabF2bwt protein and other mutants (Fig. 2, Lane 9). Degradation products were not observed for the wild-type protein or any of the mutants confirming that the

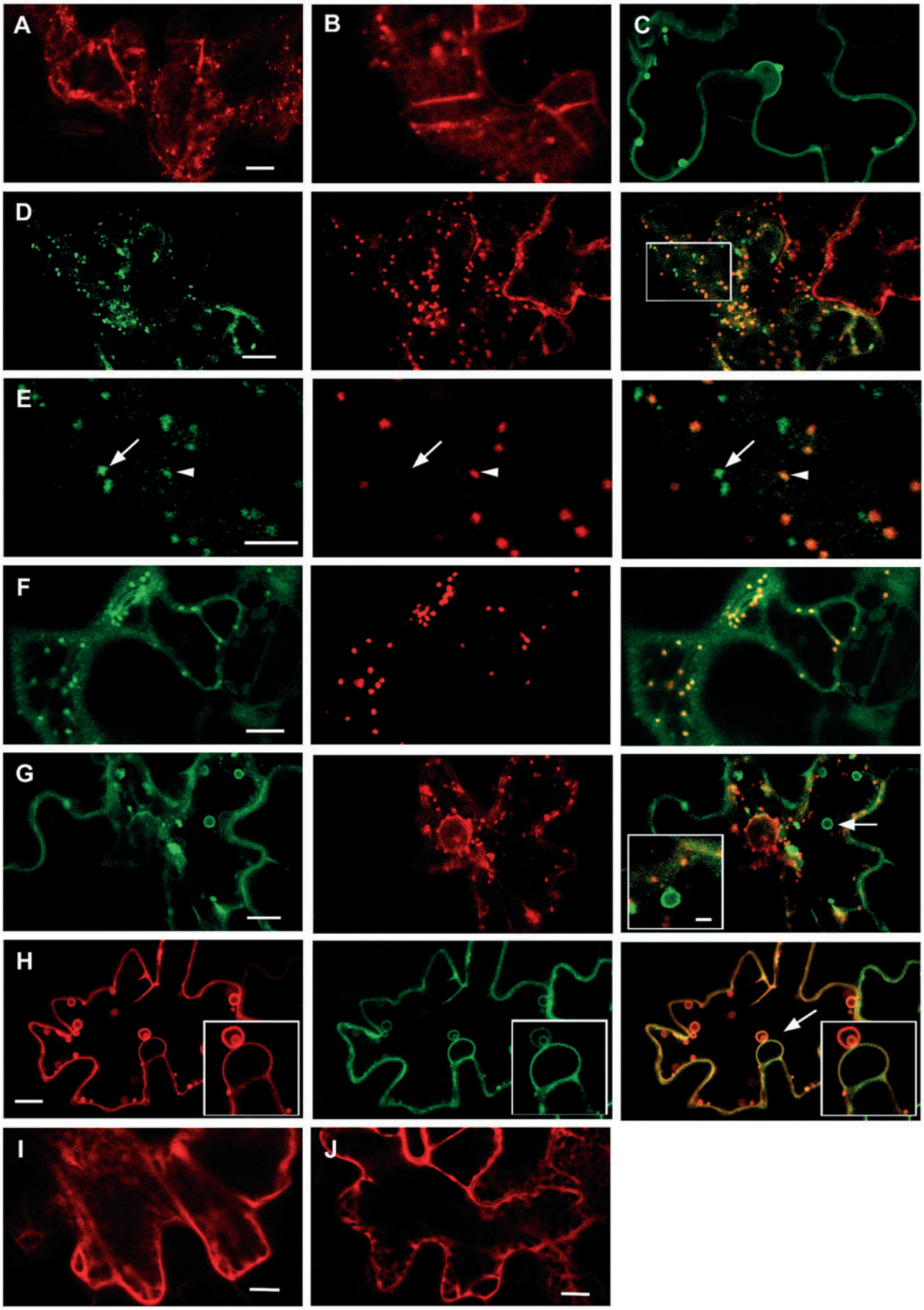
A
B
C
D
E
F
G
H
I
J

fusion proteins were stable (Fig. 2). The prevacuole marker PS1-GFP, was used as a control protein to ensure specific binding of the antibody (Fig. 2, Lanes 12 and 13). The anti-GFP antibody did not recognize epitopes within the untransformed, negative control sample (Fig. 2A, Lane 14).

Tagged *At*RabF2b localizes to the PVC

To investigate the location of YFP-*At*RabF2b[wt] punctate structures that are not distributed to the Golgi apparatus, coexpression studies were performed with PS1-GFP, a fusion created from pea BP80. Specifically, PS1-GFP is the fusion protein between GFP and the transmembrane and cytosolic domains of BP80, the pea vacuolar sorting receptor that localizes to the PVC and the trans-Golgi network (TGN) (Paris et al., 1997). When PS1-GFP was expressed alone, it localized to punctate structures that were mainly distinct from the ST-YFP-labelled Golgi representing the PVC (Fig. 3A). In another study using a very similar marker, BP80-YFP, over 90% of the BP80-YFP expression, which was distinct from the Golgi marker Mannosidase 1, colocalized with VSR antibodies (Tse et al., 2004). Additionally, immunofluorescence experiments on root tip cells stably expressing the PS1-GFP confirmed that PS1 is located in organelles containing BP80 homologues and that these rarely colocalize with the Golgi (N.P., unpublished results).

To investigate whether the population of YFP-*At*RabF2b[wt] that did not distribute to the Golgi apparatus colocalized with PS1-GFP, we coexpressed the two proteins and found that YFP-*At*RabF2b[wt] protein is indeed located at the PVC (Fig. 3B). In addition, when these two fusion proteins were expressed together, aggregates containing both proteins were formed (Fig. 3B arrow, F). When PS1-GFP was expressed with YFP-*At*RabF2b[Q69L], the fluorescent spheres normally observed in tagged-AtRabF2b[Q69L]-expressing cells disappeared (see Fig. 1C), and were replaced with large fluorescent structures (Fig. 3D). By contrast, when PS1-GFP was coexpressed with either the YFP-*At*RabF2b[S24N] or YFP-*At*RabF2b[N123I], PS1-GFP was normally distributed (Fig. 3C,E).

YFP-*At*RabF2b[S24N] colocalized with a subpopulation of PS1-GFP (Fig. 3C,G arrowheads). There was, however, always some PS1-GFP that did not colocalize with YFP-*At*RabF2b[S24N] (Fig. 3G, arrows), which may represent the PVC. This indicates that YFP-*At*RabF2b[S24N] did not prevent all the PS1-GFP from reaching this compartment.

To rule out the possibility that the fluorescent tag attached to the *At*RabF2b protein interfered with PS1-GFP, this experiment was repeated using the untagged versions of *At*RabF2b. Fluorescent aggregates were also observed in coexpression experiments of PS1-GFP and the untagged *At*RabF2b[wt] (Fig. 4A). These aggregates are similar to those seen when PS1-GFP was expressed with untagged *At*RabF2b[Q69L] (Fig. 4B). Interestingly, in cells that formed aggregates when coexpressed with the untagged constructs, the aggregates appeared more spherical and mobile than those observed when expressed with the tagged version. Cells transformed with PS1-GFP and untagged forms of *At*RabF2b[S24N] and *At*RabF2b[N123I] did not form these large accumulations (data not shown).

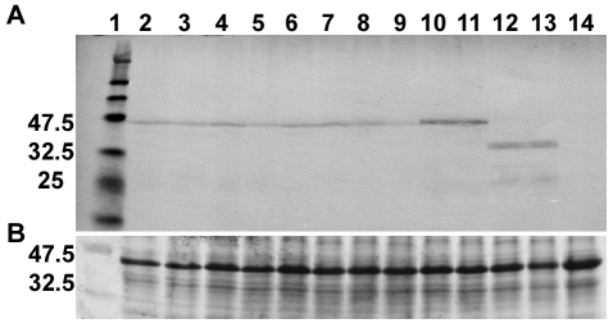

Fig. 2. Western blot of *At*RabF2b[wt] protein and chimaeras. Proteins were extracted from leaf material at 2 or 4 days after *Agrobacterium*-mediated transformation. An antibody raised against GFP was used to detect the *At*RabF2b fusion protein. (A) Lane 1, protein standard markers; lanes 2-3, *At*RabF2b[wt] day 2 and day 4; lanes 4-5, *At*RabF2b[S24N] day 2 and day 4; lanes 6-7, *At*RabF2b[Q69L] day 2 and day 4; lanes 8-9, AtRabF2b[N123I] day 2 and day 4; lanes 10-11, *At*RabF2b[C198,199S] day 2 and day 4; lanes 12-13, PS1-GFP day 2 and day 4; lane 14, untransformed control. (B) Coomassie Blue-stained gel showing equal loading of protein (lanes as above).

Aleurain-GFP punctate structures correspond to the PVC

The localization of *At*RabF2b[wt] protein to the PVC, determined by coexpression with PS1-GFP, suggests that *At*RabF2b may be involved in the vacuolar trafficking pathway. As tagged *At*RabF2b[wt] and tagged *At*RabF2b[Q69L] disrupt the normal distribution of the membrane-bound PVC marker, PS1-GFP, we asked whether *At*RabF2b and its mutant forms also affect soluble proteins that localize to the PVC.

Aleurain (aleu)-GFP has a sequence-specific vacuolar sorting determinant from petunia aleurain and is transported to the lytic vacuole (Humair et al., 2001). When aleu-GFP was expressed in tobacco leaf epidermal cells, it was only faintly detectable in the vacuole. This is consistent with the known instability of GFP in tobacco leaf vacuoles (Tamura et al., 2003). In addition to faint fluorescence in the vacuole, aleu-GFP also labelled punctate mobile structures (Fig. 5A). Upon coexpression of aleu-GFP with PS1-YFP, we verified that these punctate structures colocalized with the PVC marker (arrow,

Fig. 1. Mutations of *At*RabF2b relocalize the chimaera in tobacco leaf epidermal cells. Confocal images 2 days after *Agrobacterium* inoculation with the indicated mutants at OD_{600} 0.03. (A) YFP-*At*RabF2b[wt]. (B) YFP-*At*RabF2b[S24N]. (C) GFP-*At*RabF2b[Q69L]. (D) GFP-*At*RabF2b[wt] (green) and ST-YFP (red). (E) High magnification image of the box in D. Two populations of GFP-*At*RabF2b[wt] structures are present: punctate structures that do not colocalize with ST-YFP (arrow) and punctate structures that do (arrowhead). Bar,. (F) GFP-*At*RabF2b[S24N] (green), ST-YFP (red). Colocalization is shown in the merged image. (G) GFP-*At*RabF2b[Q69L] (green image), ST-YFP (red). GFP-*At*RabF2b[Q69L]-positive spherical structures do not colocalize with ST-YFP (arrow, merged image and insert). (H) YFP-*At*RabF2b[Q69L] (red) and BobTIP26-1::GFP (green) colocalize with BobTIP26-1::GFP on the tonoplast (arrow, merged image and insert). (I) Cytosolic labelling of YFP-*At*RabF2b[N121I]. (J) Cytosolic labelling of YFP-*At*RabF2b[C198S,199S]. Bar, 10 μm (A-D and F-J); 5 μm (E); 2 μm (inset G).

Fig. 5B). This confirms that aleu-GFP is targeted to the lytic vacuole, via the PS1-GFP-labelled PVC. We therefore used this protein as a marker to analyse the effect of *At*RabF2b fluorescent chimaeras on vacuolar trafficking.

*At*RabF2b localizes to the aleu-GFP-labelled PVC

To investigate the location and function of *At*RabF2b[wt] and mutants in the vacuolar trafficking pathway, the proteins were coexpressed with aleuGFP. When YFP-*At*RabF2b[wt] was coexpressed with aleu-GFP the YFP-*At*RabF2b[wt] labelled structures colocalized with the aleu-GFP positive PVCs (arrow, Fig. 5C). Faint YFP-*At*RabF2b[wt] structures can occasionally be observed (arrowhead, Fig. 5C). The size and distribution of the PVC compartments labelled by aleu-GFP was not affected by the presence of *At*RabF2b[wt] protein unlike the PS1-GFP-labelled PVC.

When YFP-*At*RabF2b[S24N] was coexpressed with aleu-GFP the bright, punctate, aleurain-containing PVCs did not colocalize with the Golgi-localized YFP-*At*RabF2b[S24N] (arrow, Fig. 5D). Coexpression of YFP-*At*RabF2b[Q69L] with aleu-GFP revealed that many of the spherical compartments labelled by YFP-*At*Rab[Q69L] accumulated the soluble marker aleu-GFP suggesting that these represent aberrant PVC (Fig. 5E insert). When YFP-*At*RabF2b[N123I] was coexpressed with aleu-GFP, the aleu-GFP punctate structures were not affected (Fig. 5F).

*At*RabF2b[S24N] caused secretion of vacuole-targeted aleu-GFP, which can be rescued by *At*RabF2b[wt] protein

To investigate the effect of untagged mutant forms of *At*RabF2b on the destination of aleu-GFP, images of transformed epidermal cells were taken at low magnification. When expressed alone, aleu-GFP appeared faintly in the vacuole (arrow, Fig. 6A). When untagged *At*RabF2b[wt] was expressed with aleu-GFP, there was only a slight alteration in the distribution of the aleu-GFP (Fig. 6B). Many cells still showed faint fluorescence in the vacuoles, with

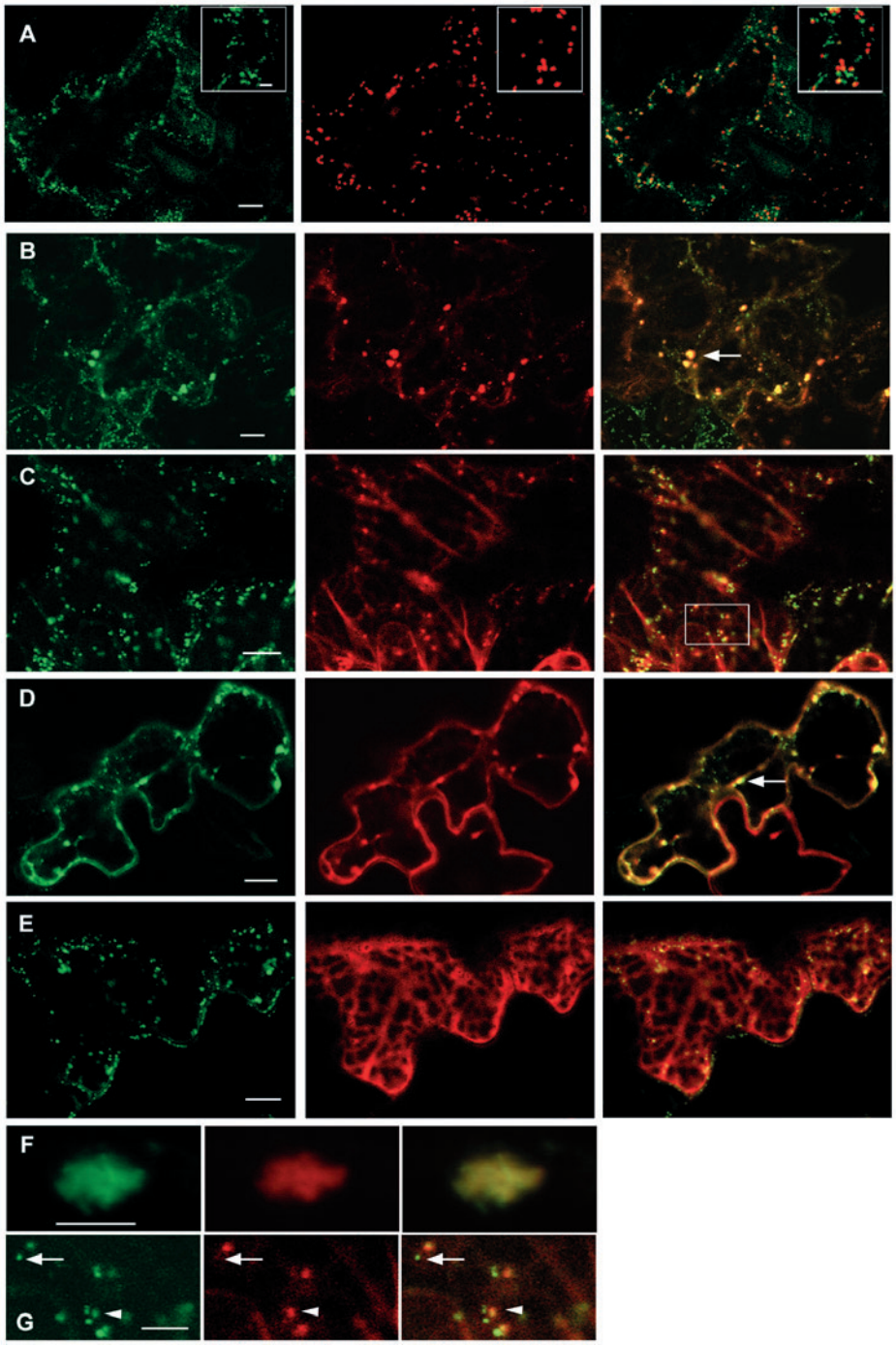

Fig. 3. *At*RabF2b-tagged chimaeras affect the normal distribution of the pre-vacuolar marker, PS1-GFP. Confocal images of tobacco leaf epidermal cells, 2 days after *Agrobacterium* inoculation with PS1-GFP (OD_{600} 0.08) and *At*RabF2b (OD_{600} 0.03). (A) PS1-GFP (green) and ST-YFP (red). The majority of PS1-GFP does not colocalize with ST-YFP (see inset taken from tangential section of the cell). (B) PS1-GFP (green) and YFP-*At*RabF2b[wt] (red) form large aggregates (arrow, merged image). (C) PS1-GFP (green) and YFP-*At*RabF2b[S24N] (red) do not form large aggregates (merged image). (D) PS1-GFP (green) and YFP-*At*RabF2b[Q69L] (red) form large aggregates (arrow, merged image). (E) PS1-GFP (green) and YFP- *At*RabF2b[N123I] (red) do not form large aggregates (merged image). (F) High magnification image of a cell expressing PS1-GFP (green) and YFP-*At*RabF2b[wt] (red), showing the nature of the aggregates. (G) High magnification of image in C. Golgi labelling of YFP-*At*RabF2b[S24N] colocalizes with a population of PS1-GFP (arrowhead), also present is a population of PS1-GFP that do not colocalize with YFP-*At*RabF2b[S24N] (arrow). Bar, 10 μm (A-E); 5 μm (F,G).

some cells exhibiting fluorescence in the apoplast presumably because of saturation of the vacuolar sorting mechanism. However, the targeting of the aleu-GFP was drastically influenced by the expression of untagged *At*RabF2b[S24N]. Rather than a weak fluorescence in the vacuole, aleu-GFP was secreted, resulting in clearly visible fluorescence in the apoplastic space (arrow, Fig. 6C). To exclude the possibility that increased apoplastic fluorescence resulted from alterations of the apoplastic environment, a secretory form of GFP was coexpressed with untagged *At*RabF2b[wt] and mutants, but no increase in apoplastic fluorescence was observed (see Fig. S1 in supplementary material). Importantly, the aleu-GFP secretion phenotype induced by *At*RabF2b[S24N] was reversed by the coexpression of *At*RabF2b[wt] protein along with *At*RabF2b[S24N] and aleu-GFP (Fig. 6D). This effect appeared to be specific to the *At*RabF2 subclass, as no rescue was observed when a member of a different subclass, the Rab1/Ypt1-related *At*RabD2a, was coexpressed with *At*RabF2b[S24N] and aleu-GFP (Fig. 6E).

To quantify these results, we counted the number of cells in which at least half the apoplast was visibly decorated with aleu-GFP fluorescence. Data was collected from three independent experiments and cells expressing fluorescent in the apoplast, in eight fields of view per construct, were counted (Fig. 6F). ANOVA indicated that the number of cells with aleu-GFP visible in the apoplast when coexpressed with *At*RabF2b[S24N] was significantly different ($P<0.05$) to the number obtained with aleu-GFP alone, aleu-GFP and *At*RabF2b[wt] and when the dominant-negative effect was rescued by coexpression with the *At*RabF2b[wt] protein. Fig. 6F also indicates that the rescue of the dominant-negative phenotype by coexpression with wild-type protein was 90% effective. Efficient rescue of the dominant negative phenotype by *At*RabF2b[wt], suggests that secretion of aleu-GFP to the apoplast results from loss of *At*RabF2b function in these cells.

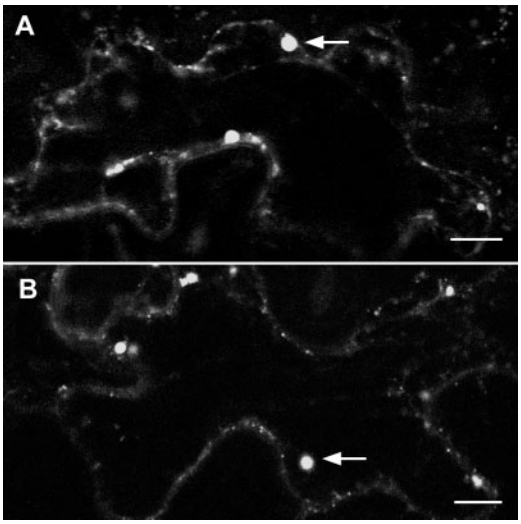

Fig. 4. Untagged *At*RabF2b chimaeras also affect the normal distribution of the pre-vacuolar marker, PS1-GFP. Confocal images of tobacco leaf epidermal cells, 2 days after *Agrobacterium* inoculation with PS1-GFP (OD_{600} 0.08) and untagged-*At*RabF2b (OD_{600} 0.03). (A) Representative cell transformed with PS1-GFP and untagged *At*RabF2b[wt]. Large aggregates are present in the absence of the fluorescent tag (arrow). (B) Representative cell transformed with PS1-GFP and untagged *At*RabF2b[Q69L]. Again, large aggregates containing PS1-GFP are present (arrow). Bar, 10 μm.

Fluorescent-tagged *At*RabF2b[wt] affects the normal transport of aleu-GFP

To investigate the effect of the fluorescent tag on the function of the *At*RabF2b, low magnification images were taken of YFP-*At*RabF2b[wt], YFP-*At*RabF2b[S24N] and YFP-*At*RabF2b[C198,199S], coexpressed with aleu-GFP (Fig. 7). The addition of the fluorescent protein to *At*RabF2b[wt] caused increased secretion of aleu-GFP to the apoplast compared to the untagged version (cf. Fig. 6B and Fig. 7D). YFP-*At*RabF2b[S24N] did not appear to cause as much secretion as the untagged version (cf. Fig. 7E and B). Interestingly, when YFP-*At*RabF2b[C198,199S], which lacks a functional isoprenylation motif, was expressed with aleu-GFP it did not affect the transport of the aleu-GFP (Fig. 7F) indicating that membrane association or association with an interactor such as RabGDI is essential for tagged *At*RabF2b to alter trafficking of aleu-GFP.

Discussion

In mammalian cells, Rab5 is involved in the endocytic pathway and in yeast, homologues are involved in both the endocytic and vacuolar trafficking pathways (Bucci et al., 1992; Olkkonen et al., 1993; Singer-Kruger et al., 1994). The corresponding subclasses in plants, *At*RabF1 and *At*RabF2, have been implicated in both the endocytic and vacuolar trafficking pathways (Bolte et al., 2004a; Geldner et al., 2003; Grebe et al., 2003; Sohn et al., 2003; Ueda et al., 2001). GFP-*At*RabF2b has been localized to FM4-64-positive endosomal compartments whose structure was affected by the gnom mutation, which interferes with recycling of several plasma membrane proteins (Ueda et al., 2001; Geldner et al., 2003).

*At*RabF2b[wt] localizes to the PVC and Golgi

GFP or YFP fusion proteins were expressed with a variety of markers in the tobacco leaf transient expression system. Tagged-*At*RabF2b[wt] colocalized predominantly with the PVC marker, PS1-GFP. However, a proportion of the *At*RabF2b[wt] protein was localized on ST-YFP-labelled Golgi bodies. YFP-*At*RabF2b[wt] also altered the appearance of PS1-GFP-labelled compartments and caused secretion of aleu-GFP. It is thus likely that the major *At*RabF2b-labelled compartment represents the PVC on the lytic vacuole pathway because the small punctate structures labelled by the lytic-vacuole marker aleu-GFP could be labelled by PS1-YFP and YFP-*At*RabF2b without noticeable alteration in their appearance. Previous findings in *Arabidopsis* protoplasts, suggested an endosomal or prevacuolar location of the *At*RabF2b[wt] protein, based on studies with FM4-64 (Ueda et al., 2001). These findings may be reconciled by the demonstration that in tobacco BY2 suspension cells, BP80-YFP colocalizes with anti-VSR labelling and that this compartment is additionally labelled with FM4-64 (Tse et al., 2004).

Confusion regarding the identity of the structures labelled by FM4-64 has resulted in further investigation into the

relationship between endosomes and PVCs. The mechanism by which this dye is taken up into plant cells is not clear and concerns regarding its specificity as an endosomal marker have been voiced, as studies in tobacco BY2 suspension cells have suggested that the dye can also label the Golgi apparatus at similar time points to the labelling of putative endosomes (Bolte et al., 2004b). By contrast, in the same system, only 11% of Golgi stacks were labelled by FM4-64 at a time when 85% of BP80-YFP-labelled PVCs were labelled by the dye (Tse et al., 2004). From our studies, we propose that *At*RabF2b labels the PVC, which is probably spatially, if not temporally, the same compartment as the late endosome. More importantly, regardless of the nature of this common compartment, our evidence to date suggests that *At*RabF2b is involved in the vacuole trafficking pathway, as the dominant-negative mutant affects the trafficking of a vacuole-targeted protein. It must be noted that neither *At*RabF2a nor *At*RabF2b have yet been shown to localize to a compartment that is unambiguously an endosome (i.e. one that carries an endocytosed plasma membrane protein) nor known to be required for any trafficking event on the endocytic pathway. In our study, we have not identified any effects of *At*RabF2b[wt] or mutants on plasma membrane proteins (*Nt*AQP1-GFP, BP22-GFP, PMA4-GFP) (A.M.K., unpublished) (Brandizzi et al., 2002a; Lefebvre et al., 2004) that traffic on the Golgi-plasma membrane pathway and may be subject to endocytic events.

As well as localizing to the PVC, we show that *At*RabF2b[wt] also partially distributes to the Golgi apparatus. We hypothesize that *At*RabF2b may cycle between the Golgi and PVC in a similar fashion to BP80 (Fig. 8). These findings are reinforced by the fact that the GDP-bound *At*RabF2b[S24N] is restricted to the Golgi and the GTP-bound form *At*RabF2b[Q69L] localizes to PVCs (Fig. 8).

BP80 is believed to cycle between the Golgi and the PVC where it functions in sorting proteins such as aleurain, which have sequence-specific vacuolar sorting signals to the lytic vacuole. The native pea BP80 is found in the prevacuole and in regions budding off the trans Golgi, probably the TGN, in the pea cotyledon (Paris et al., 1997). BP80 and homologues were also observed to accumulate

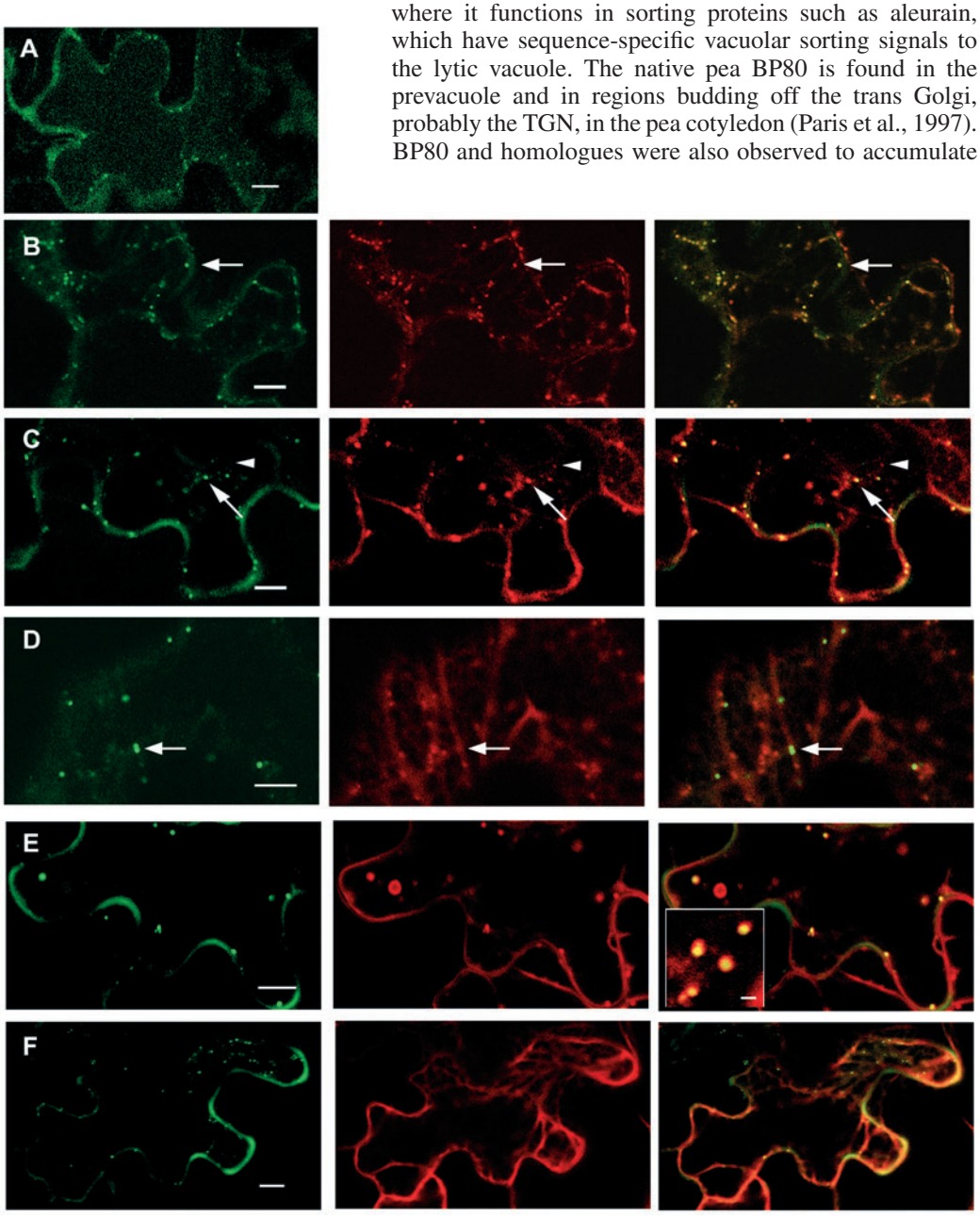

Fig. 5. *At*RabF2b localizes to the aleu-GFP-labelled PVC. Confocal images of tobacco leaf epidermal cells, 2 days after *Agrobacterium* inoculation with aleu-GFP (OD_{600} 0.1) and *At*RabF2b (OD_{600} 0.03). (A) Aleu-GFP faintly fluoresces in the vacuole and also labels small punctate structures. (B) Aleu-GFP (green) and PS1-YFP (red). Aleu-GFP localizes to the PVC compartment also labelled with PS1-YFP (arrow). (C) Aleu-GFP (green), YFP-*At*RabF2b[wt]-labelled structures colocalize with PVC-containing aleurain (arrow). Faint YFP- *At*RabF2b[wt] structures are still visible (arrowhead). (D) Aleu-GFP (green) and YFP-*At*RabF2b[S24N] (red). Bright, punctate aleurain structures do not colocalize with *At*RabF2b[S24N] (arrow). (E) Aleu-GFP (green) and YFP-*At*RabF2b[Q69L] (red). Aleu-GFP accumulates in *At*RabF2b[Q69L] spheres (insert, merged image). Insert image was taken from an additional cell, which clearly showed aleu-GFP accumulating within the spheres. (F) Aleu-GFP (green) and YFP-*At*RabF2b[N123I] (red). Aleurain-positive pre-vacuoles are not affected by the presence of YFP-*At*RabF2b[N123I]. Bar, 10 μm (A-F); 2 μm in insert (E).

preferentially in the PVC with only a little found in the TGN (Li et al., 2002). This distribution was recently confirmed in tobacco BY2 suspension cells using a BP80-YFP construct similar to the one used in this study: a fluorescent protein plus the transmembrane and the cytosolic domains of peaBP80 (Tse et al., 2004). We also performed immunofluorescence experiments on root tip cells stably expressing the PS1 construct in its GFP version and we confirmed that PS1 is localized in organelles containing tobacco BP80 homologues (N.P., unpublished data).

Mutations in nucleotide-binding regions alter the location of *At*RabF2b

The locations of the GDP- and GTP-bound forms of *At*RabF2b suggest that the protein is recruited to Golgi membranes and transported to the PVC. In the tobacco leaf epidermal system, transiently expressed GFP-*At*RabF2b[S24N] colocalizes completely with the Golgi marker ST-YFP (Fig. 8). Punctate structures were also observed in *Arabidopsis* protoplasts expressing RFP-tagged *At*RabF2a[S24N] but in this study it was suggested that these structures were PVCs (Sohn et al., 2003). Although these differences may be related to the different experimental material used, it should be noted that there is no colocalization or fractionation data to support the suggestion that *At*RabF2a[S24N] localizes to the PVC in *Arabidopsis* protoplasts and its location in intact *Arabidopsis* cells has not been reported (Sohn et al., 2003).

It is interesting that a substantial fraction of the YFP-*At*RabF2b[S24N], which is predicted to preferentially bind GDP, is located on the Golgi rather than in the cytosol. This indicates that the protein is recruited to this organelle from the cytosol. The GDP-bound form of Rab protein is mainly cytosolic and associated with the GDP dissociation inhibitor (GDI). It has been shown that it is possible for GDI to be membrane-bound independently of the Rab in *Saccharomyces cerevisiae* (Luan et al., 1999). Similarly, in tobacco leaf epidermal cells *At*RabF2b[S24N] may associate with membrane-associated RabGDI. However, we have found that two other Golgi-localized Rabs are fully cytosolic when the equivalent S24N mutation is introduced (U.N., L. Camacho and I.M., unpublished results) so *At*RabF2b[S24N] would have to bind preferentially to Golgi-localized RabGDI to account for its location. Alternatively, the GDP-bound form of the Rab protein may interact specifically with a membrane-bound partner after release from GDI and recruitment to the membrane (Sivars et al., 2003; Soldati et al., 1994; Ullrich et al., 1994) or it may remain associated with the membrane as proposed recently for mammalian Rab11 (Pasqualato et al., 2004). As the dominant inhibitory characteristics of this mutant probably result from sequestration of a specific nucleotide exchange factor, another possibility is that a Golgi-localized nucleotide exchange factor recruits significant amounts of *At*RabF2b[S24N] to the Golgi membranes.

By contrast, tagged-*At*RabF2b[Q69L], which is predicted to be GTPase deficient, labels 1-2 μm diameter spherical structures and the tonoplast (Fig. 8). Ueda et al. (Ueda et al., 2001) showed that *Arabidopsis* protoplasts expressing tagged

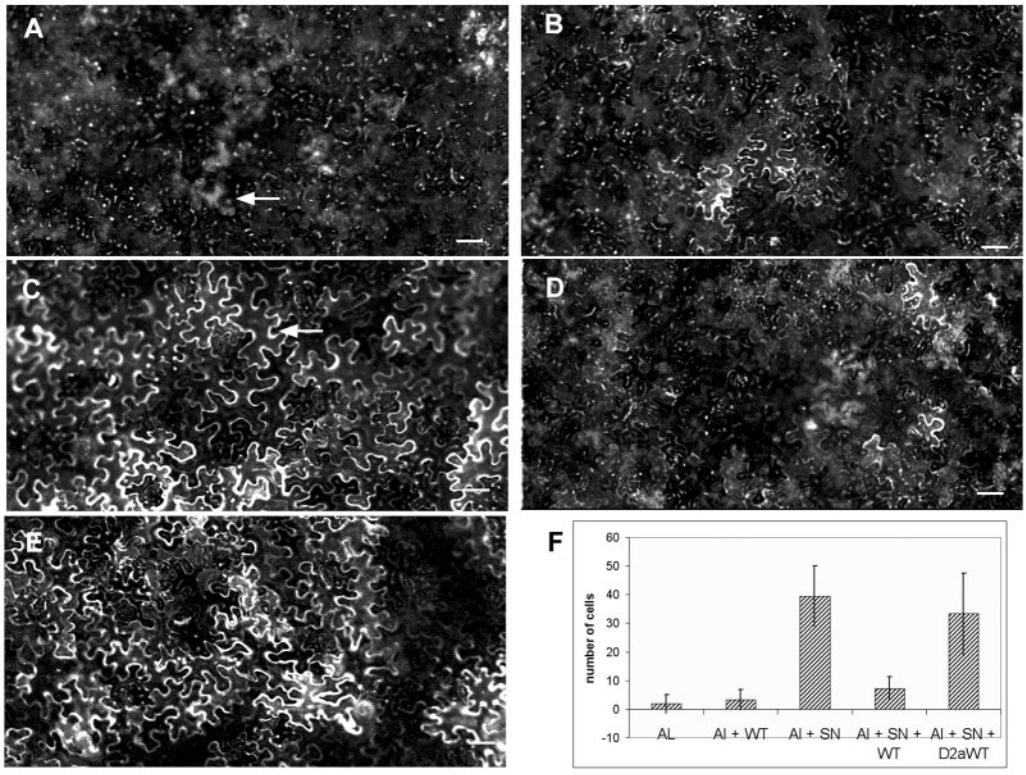

Fig. 6. Untagged dominant-negative mutant causes secretion of vacuole-targeted aleu-GFP, which can be rescued by *At*RabF2b[wt]. Confocal images of tobacco leaf epidermal cells, 48-52 hours after *Agrobacterium* inoculation with aleu-GFP (OD_{600} 0.1) and untagged-*At*RabF2b and AtRabD2a (OD_{600} 0.05). (A) With aleu-GFP alone, faint fluorescence is visible in some vacuoles (arrow). (B) In cells expressing aleu-GFP and *At*RabF2b[wt], the fluorescent pattern of aleu-GFP is not affected. (C) With aleu-GFP and *At*RabF2b[S24N], location of aleu-GFP is drastically altered by the dominant-negative mutant as fluorescence is clearly visible in the apoplast (arrow). (D) With aleu-GFP, *At*RabF2b[S24N] and *At*RabF2b[wt], *At*RabF2b[wt] has rescued the effect of the dominant-negative mutant on the localization of aleu-GFP. Very few cells secreting GFP to the apoplastic space are present. (E) Cells expressing aleu-GFP, *At*RabF2b[S24N] and *At*RabD2a; expression of another Rab protein does not rescue the phenotype of aleu-GFP induced by *At*RabF2b[S24N] as seen with *At*RabF2b[wt]. Bar, 50 μm. (F) Analysis of cells with GFP visible in the apoplast. Data represent mean±s.d. of three independent experiments (eight fields of view per construct) of cells secreting to the apoplast. AL, aleu-GFP; WT, untagged *At*RabF2b[wt]; SN, untagged *At*RabF2b[S24N]; D2aWT, untagged *At*RabD2a[wt].

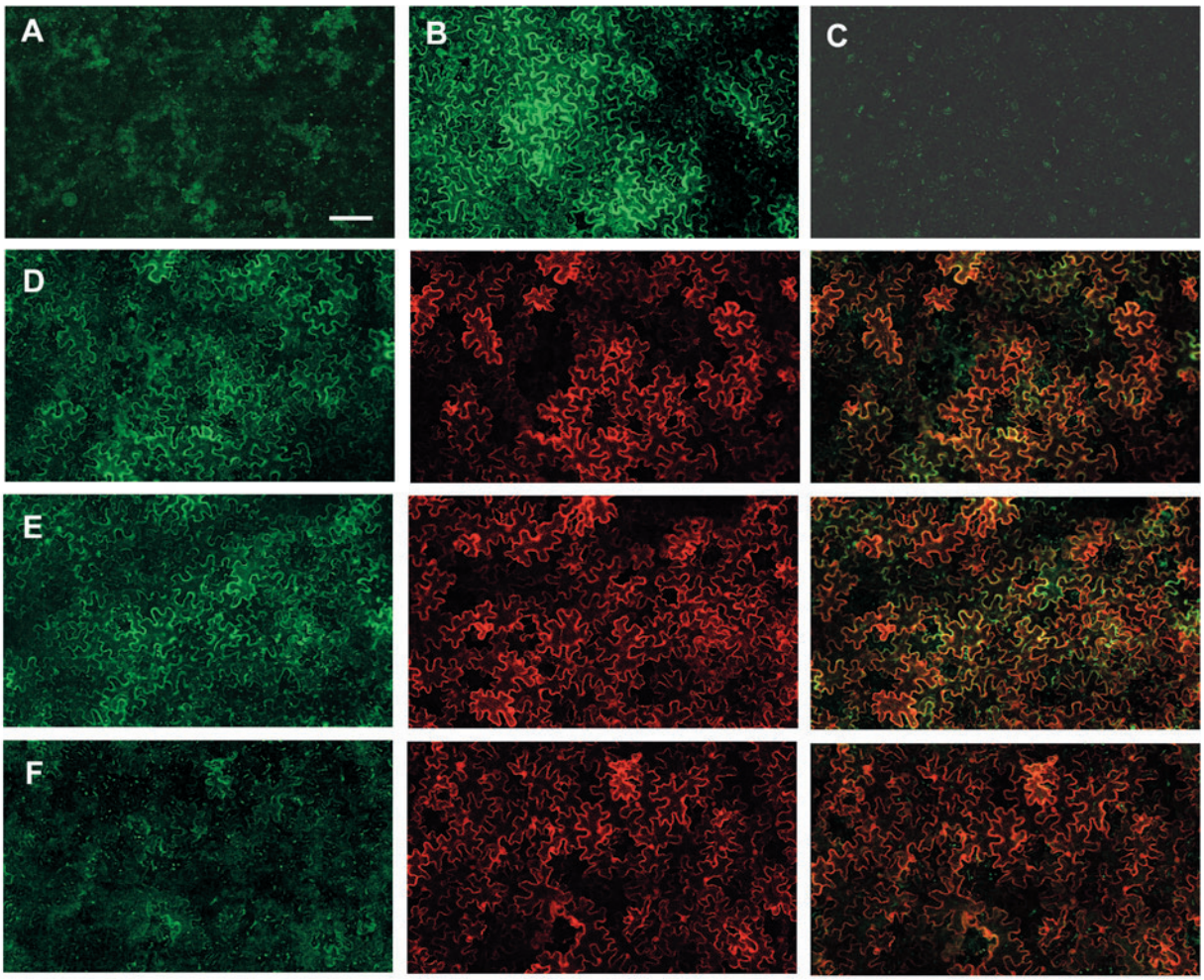

Fig. 7. Effect of fluorescent-tagged *At*RabF2b on trafficking of aleu-GFP. Confocal images of tobacco leaf epidermal cells, 48-52 hours after *Agrobacterium* inoculation with aleu-GFP (OD_{600} 0.1) and tagged-*At*RabF2b (OD_{600} 0.05). (A) With aleu-GFP alone, faint fluorescence is visible in some vacuoles. (B) Aleu-GFP and untagged *At*RabF2b[S24N]. (C) Untransformed leaf. (D) Aleu-GFP (green) and YFP-*At*RabF2b[wt] (red) expression, showing aleu-GFP is secreted to the apoplast. (E) Aleu-GFP (green) and YFP-*At*RabF2b[S24N] (red) expression; aleu-GFP is secreted at similar levels to D. (F) aleu-GFP(green) and YFP-*At*RabF2b[C198, 199S] (red) expression; aleu-GFP is not secreted to the apoplast. Bar, 50 μm.

*At*RabF2b[Q69L] also exhibited unusually large spherical structures that stained with FM4-64 and suggested that these represented swollen endosomes. Two lines of evidence in our study suggest that the spherical structures observed with tagged-*At*RabF2b[Q69L] may represent a common PVC/endosome compartment. First, the fusion colocalizes with PS1-GFP, but not with a Golgi marker, and appears to alter the morphology of the *At*RabF2b[Q69L]-induced spheres in large immobile aggregates. Second, the majority of the spheres accumulated the soluble vacuolar cargo molecule aleu-GFP. As the GTPase-deficient mutant is likely to recycle to the cytoplasm less efficiently than the wild type, we suggest that the PVC is the normal destination of *At*RabF2b following recruitment to the Golgi and activation to the GTP-bound form. Furthermore, as the GTPase-deficient mutant is predicted to remain longer than the wild type in its active GTP-bound configuration, it may cause swelling of the PVC by promoting excessive membrane fusion in a manner analogous to the action of mammalian Rab5[Q79L] on early endosomes (Stenmark et al., 1994). The accumulation of YFP-A*t*RabF2b[Q69L] on the tonoplast may be another consequence of reduced GTP hydrolysis. As we have shown that *At*RabF2b acts on a pathway from the Golgi to a PVC, slow recycling of the A*t*RabF2b[Q69L] mutant off the membrane of this prevacuole may result in its transport by default to the vacuole and its stable accumulation on the tonoplast. This hypothesis is supported by recent observations on Ytp1p in yeast (De Antoni et al., 2002). These authors showed first that although the in vivo hydrolysis rate of Ypt1p carrying the equivalent QL mutation is 100-fold lower than that of the wild type, GTP hydrolysis may still be catalysed 104-fold by the cognate GTPase-activating factors (GAP) activity. Secondly, it was shown that Ypt1-specific GAP proteins exhibit distinct subcellular localizations rather than a general cytoplasmic distribution (Bortoluzzi et al., 1996; Cuif et al., 1999; De Antoni et al., 2002). If *At*RabF2b and its cognate GAP exhibit the same characteristics, the Q69L mutant may still recycle slowly off the prevacuolar membranes owing to a reduced

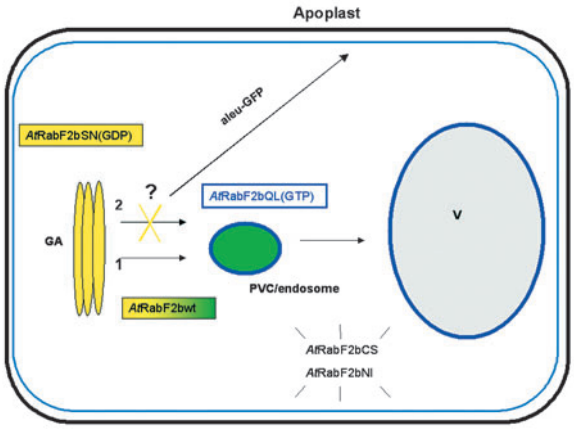

Fig. 8. Location and putative function of *At*RabF2b in tobacco leaf epidermal cells. The location of *At*RabF2b[wt] on the Golgi apparatus, PVC, and the effect of the dominant-negative mutant on the vacuole targeted protein aleurain-GFP suggest its role in GA to PVC trafficking. The tagged GDP locked mutant *At*RabF2b[S24N] localizes entirely to the GA whereas the tagged-GTP locked mutant *At*RabF2b[Q69L] localizes to spherical structures at the PVC and also to the tonoplast. (1) Aleu-GFP trafficks through the PVC en route to the vacuole. (2) When untagged *At*RAbF2b[S24N] is coexpressed with aleu-GFP, a proportion of the aleu-GFP is secreted to the apoplast. Tagged *At*RabF2b[C198,199S] and tagged *At*RabF2b[N123I] are entirely cytosolic. aleu-GFP, aleurain-GFP; GA, Golgi apparatus; PVC, prevacuole compartment; V, vacuole.

GAP-catalysed hydrolysis rate, but once it is transported to a membrane such as the tonoplast that lacks the cognate GAP it will be recycled 10,000 times less efficiently and will accumulate at this membrane.

Redirecting the vacuolar pathway

Our observation that dominant inhibitory *At*RabF2b[S24N] causes the vacuolar marker aleu-GFP to be redirected to the cell surface in tobacco leaf epidermal cells indicates that this mutant most probably interferes in normal vacuolar sorting or trafficking (Fig. 8). Importantly, we also show that normal vacuolar trafficking of aleu-GFP can be effectively (~90%) restored by coexpression of the dominant inhibitory mutant with wild-type *At*RabF2b but not with an unrelated Rab GTPase. Therefore, we propose that the vacuolar-sorting defect probably results from loss of *At*RabF2b function in these cells and that *At*RabF2b is required for normal transport on the vacuolar pathway followed by aleu-GFP.

Despite the mis-sorting of aleu-GFP to the apoplast in the presence of *At*RabF2b[S24N] we still observe this marker in punctate structures that resemble the PVC compartments labelled in control cells. This may reflect inhibition of membrane traffic at or after the PVC. However, as the protein appears to associate with the Golgi apparatus in its GDP-bound form, it seems likely that the dominant-negative mutant acts at this organelle. The continued presence of aleu-GFP in the PVC may then simply reflect incomplete inhibition of traffic along the vacuolar pathway as observed with *At*RabF2a (Sohn et al., 2003). Alternatively, as the Golgi is the site of sorting into the lytic vacuolar pathway, when *At*RabF2b function is impaired it may be either that aleu-GFP becomes diverted through alternative but morphologically similar PVCs or that post-Golgi transport intermediates are not programmed with the necessary targeting information at the Golgi and thus accumulate. Inefficient targeting of post-Golgi intermediates could lead secondarily to disruption of vacuolar sorting or traffic owing to a failure to recycle essential membrane components.

Our observations with *At*RabF2b[S24N] are similar to the results reported by Sohn et al. (Sohn et al., 2003) who worked with the other member of the RabF2 subclass in *Arabidopsis*, *At*RabF2a (Rha1). These authors showed that YFP- or HA-tagged versions of *At*RabF2a[S24N] caused 30-40% of the lytic vacuole markers sporamin-GFP and aleu-GFP to be secreted from *Arabidopsis* protoplasts. In the case of *At*RabF2a, the vacuolar-sorting defect induced by the tagged S24N mutant appears to be only inefficiently rescued (~40%) by coexpression with wild-type *At*RabF2a. Although this result suggests that the tagged dominant-negative *At*RabF2a mutant may inhibit an activity that cannot be supplied by the wild-type protein, its interpretation is difficult because the vacuolar sorting efficiency of control protoplasts expressing wild-type *At*RabF2a was not reported (Sohn et al., 2003) nor was the rescue attempted with untagged mutant protein (see below). Our data now provide clear evidence for involvement of the RabF2 subclass, particularly *At*RabF2b, in vacuolar traffic.

In the higher plant Rab family, the Rab5-related RabF clade has been subdivided into two subclasses, *At*RabF1 and *At*RabF2 that may perform distinct functions (Perierra-Leal and Seabra, 2001; Rutherford and Moore, 2002). The *At*RabF1 subclass is unique amongst Rab proteins in having N-terminal myristoylation and palmitoylation rather than C-terminal prenylation (Bolte et al., 2000; Borg et al., 1997; Ueda et al., 2001). In contrast to *At*RabF2a[S24N], an epitope-tagged form of the *Arabidopsis* RabF1 protein (*At*RabF1; Ara6) carrying the equivalent serine-to-asparagine substitution (AtRabF1[S47N]), did not cause secretion of a vacuolar marker when expressed in *Arabidopsis* protoplasts (Sohn et al., 2003). However, m-Rab$_{mc}$, a homologue of *At*RabF1 from *Mesembryanthemum crystallinum*, also localizes on the PVC and partially on the Golgi of *Arabidopsis* protoplasts and transient expression of a dominant inhibitory mutant (in this case N147I) prevents the accumulation of aleu-GFP in the central vacuole (Bolte et al., 2004a). In these respects, its properties are more similar to *At*RabF2b in tobacco leaf epidermal cells (this study) and *At*RabF2a in *Arabidopsis* protoplasts than to *At*RabF1 (Sohn et al., 2003). It remains to be established whether these differing observations reflect differences in the properties of the RabF1 proteins of these two species, in the assay method, or in the effect of the mutations introduced in each case.

Fluorescent-tagged *At*RabF2b[wt] causes secretion of aleu-GFP whereas tagged *At*RabF2b[C198,199S] does not

When untagged *At*RabF2b[wt] was coexpressed with aleu-GFP no effects were observed on the normal trafficking of aleu-GFP. By contrast, coexpression of fluorescently tagged *At*RabF2b[wt] caused mis-sorting of aleu-GFP to the apoplast. This activity, which was similar to that of the dominant-negative S24N mutant, was apparently dependent upon

membrane attachment as no secretion of aleu-GFP was detected upon coexpression with YFP-*At*RabF2b[C198,199S]. This behaviour is not a general property of tagged Rab proteins as we did not observe similar effects with GFP-tagged Rabs of the RabB, RabH or RabE subclasses that all localize to the Golgi (J. N. Johansen, L. Camacho and I.M., unpublished data). Thus, addition of YFP to the N-terminus of *At*RabF2b appears to create a dominant inhibitory protein that can associate with the PVC and Golgi where it interferes with vacuolar sorting. At present, it is not clear whether mis-sorting results from specific inhibition of normal *At*RabF2 function. A previous study reported that RFP- or HA-tagged *At*RabF2a[S24N] prevented the accumulation of sporamin-GFP or aleurain-GFP in the central vacuole of *Arabidopsis* protoplasts whereas RFP-tagged mutants that were predicted to be dysfunctional (T42A and C198,199S) did not (Sohn et al., 2003). However, the effects of *At*RabF2a[wt], tagged or untagged, on vacuolar accumulation of these markers or their secretion into the medium were not reported. Consequently, it remains unclear whether addition of the tag per se has a similar effect on *At*RabF2a and *At*RabF2b; however, processing of spo-GFP to a 30 kDa form proceeded normally in the presence of HA-tagged *At*RabF2a[wt] which may indicate that its trafficking was unaffected (Sohn et al., 2003).

In conclusion, we show here that the *At*RabF2 subclass, more precisely *At*RabF2b, is required for the sorting of a vacuolar marker to the central vacuole of tobacco leaf epidermal cells via the PVC most probably by cycling between the Golgi and PVC compartments.

We would like to thank Nathalie Leborgne-Castel for pDR1303-BobTIP26-1::GFP. This work was supported by an Oxford Brookes University studentship to A.M.K. and BBSRC grants to I.M. and C.H.

References

Ausubel, F., Brent, R., Kingston, R. E., Moore, J. G., Seidman, J. G., Smith, J. A. and Struhl, J. G. (1999). *Current Protocols in Molecular Biology*. New York, NY: John Wiley.

Batoko, H., Zheng, H., Hawes, C. and Moore, I. (2000). A Rab1 GTPase is required for transport between the endoplasmic reticulum and golgi apparatus for normal golgi movement in plants. *Plant Cell* **12**, 2201-2217.

Boevink, P., Oparka, K., Santa Cruz, S., Martin, B., Betteridge, A. and Hawes, C. (1998). Stacks on tracks: the plant Golgi apparatus traffics on an actin/ER network. *Plant J.* **15**, 441-447.

Bolte, S., Schiene, K. and Dietz, K. (2000). Characterization of a small GTP binding protein of the rab 5 family in *Mesembryanthemum crystallinum* with increased level of expression during early salt stress. *Plant Mol. Biol.* **42**, 923-936.

Bolte, S., Brown, S. and Satiat-Jeunemaitre, B. (2004a). The N-myristoylated Rab-GTPase m-Rab_{mc} is involved in the post-Golgi trafficking events to the lytic vacuole in plant cells. *J. Cell Sci.* **117**, 943-954.

Bolte, S., Talbot, C., Boutte, Y., Catrice, O., Read, N. and Satiat-Jeunemaitre, B. (2004b). FM-dyes as experimental probes for dissecting vesicle trafficking in living plant cells. *J. Microsc.* **214**, 159-173.

Borg, S., Brandstrup, B., Jensen, T. J. and Poulsen, C. (1997). Identification of new protein species among 33 different small GTP-binding proteins encoded by cDNAs from Lotus japonicus, and expression of corresponding mRNAs in developing root nodules. *Plant J.* **11**, 237-250.

Bortoluzzi, M. N., Cormont, M., Gautier, N., VanObberghen, E. and LeMarchandBrustel, Y. (1996). GTPase activating protein activity for Rab4 is enriched in the plasma membrane of 3T3-L1 adipocytes. Possible involvement in the regulation of Rab4 subcellular localization. *Diabetologia* **39**, 899-906.

Bourne, H. R., Sanders, D. A. and McCormick, F. (1991). The GTPase superfamily conserved structure and molecular mechanisms. *Nature* **349**, 117-127.

Brandizzi, F., Frangne, N., Marc-Martin, S., Hawes, C., Neuhaus, J. and Paris, N. (2002a). The destination for single-pass membrane proteins is influenced markedly by the length of the hydrophobic domain. *Plant Cell* **14**, 1077-1092.

Brandizzi, F., Snapp, E., Roberts, A., Lippincott-Schwartz, J. and Hawes, C. (2002b). Membrane protein transport between the ER and Golgi in Tobacco leaves is energy dependent but cytoskeleton independence: evidence from selective photobleaching. *Plant Cell* **14**, 1293-1309.

Bucci, C., Parton, R. G., Mather, I. H., Stunnenberg, H., Simons, K., Hoflack, B. and Zerial, M. (1992). The small GTPase rab5 functions as a regulatory factor in the early endocytic pathway. *Cell* **70**, 715-728.

Cormack, B. P., Valdivia, R. H. and Falkow, S. (1996). FACS-optimized mutants of the green fluorescent protein (GFP). *Gene* **173**, 33-38.

Cuif, M. H., Possmayer, F., Zander, H., Bordes, N., Jollivet, F., Couedel-Courteille, A., Janoueix-Lerosey, I., Langsley, G., Bornens, M. and Goud, B. (1999). Characterization of GAPCenA, a GTPase activating protein for Rab6, part of which associates with the centrosome. *EMBO J.* **18**, 1772-1782.

De Antoni, A., Schmitzova, J., Trepte, H. H., Gallwitz, D. and Albert, S. (2002). Significance of GTP hydrolysis in Ypt1p-regulated endoplasmic reticulum to Golgi transport revealed by the analysis of two novel Ypt-GAPs. *J. Biol. Chem.* **277**, 41023-41031.

Geelen, D., Leyman, B., Batoko, H., di Sansebastiano, G. P., Moore, I., Blatt, M. R. and di Sansabastiano, G. P. (2002). The abscisic acid-related SNARE homolog NtSyr1 contributes to secretion and growth: evidence from competition with its cytosolic domain. *Plant Cell* **14**, 387-406.

Geldner, N., Anders, N., Wolters, H., Keicher, J., Kornberger, W., Muller, P., Delbarre, A., Ueda, T., Nakano, A. and Jurgens, G. (2003). The *Arabidopsis* GNOM ARF-GEF mediates endosomal recycling, auxin transport, and auxin-dependent plant growth. *Cell* **112**, 219-230.

Grebe, M., Xu, J., Mobius, W., Ueda, T., Nakano, A., Geuze, H. J., Rook, M. B. and Scheres, B. (2003). *Arabidopsis* sterol endocytosis involved actin-mediated trafficking via Ara6-positive early endosomes. *Curr. Biol.* **13**, 1378-1387.

Höfgen, R. and Willmitzer, L. (1988). Storage of competent cells for Agrobacterium. transformation. *Nucleic Acids Res.* **16**, 9877.

Humair, D., Felipe, D. H., Neuhaus, J.-M. and Paris, N. (2001). Demonstration in Yeast of the function of BP-80, a putative plant vacuolar sorting receptor. *Plant Cell* **13**, 781-792.

Lefebvre, B., Batoko, H., Duby, G. and Boutry, B. (2004). Targeting of a *Nicotiana plumbaginifolia* H^+-ATPase to the plasma membrane is not by default and requires cytosolic structural determinants. *Plant Cell* **16**, 1772-1789.

Li, Y. B., Rogers, S. W., Tse, Y. C., Lo, S. W., Sun, S. S., Jauh, G. Y. and Jiang, L. (2002). BP-80 and homologs are concentrated on post-Golgi, probable lytic prevacuolar compartments. *Plant Cell Physiol.* **43**, 726-742.

Luan, P., Balch, W. E., Emr, S. D. and Burd, C. G. (1999). Molecular dissection of guanine nucleotide dissociation inhibitor function in vivo. *J. Biol. Chem.* **274**, 14806-14817.

Nuoffer, C. and Balch, W. E. (1994). GTPases: multifunctional molecular switches regulating vesicular traffic. *Annu. Rev. Biochem.* **63**, 949-990.

Olkkonen, V. M. and Stenmark, H. (1997). Role of Rab GTPases in membrane traffic. *Int. Rev. Cytol.* **176**, 1-67.

Olkkonen, V. M., Dupree, P., Killisch, I., Lutcke, A., Zerial, M. and Simons, K. (1993). Molecular cloning and subcellular localization of three GTP-binding proteins of the rab superfamily. *J. Cell Sci.* **106**, 1249-1261.

Paris, N., Rogers, S. W., Jiang, L., Kirsch, T., Beevers, L., Phillips, T. E. and Rogers, J. C. (1997). Molecular cloning and further characterization of a probable plant vacuolar sorting receptor. *Plant Physiol.* **115**, 29-39.

Pasqualato, S., Senic-Matuglia, F., Renault, L., Goud, B., Salamero, J. and Cherfils, J. (2004). The structural GDP/GTP cycle of Rab11 reveals a novel interface involved in the dynamics of recycling endosomes. *J. Biol. Chem.* **279**, 11480-11488.

Pereira-Leal, J. B. and Seabra, M. C. (2001). Evolution of the Rab family of small GTP-binding proteins. *J. Mol. Biol.* **313**, 889-901.

Reisen, D., Leborgne-Castel, N., Ozalp, C., Chaumont, F. and Marty, F. (2003). Expression of a cauliflower tonoplast aquaporin tagged with GFP in tobacco suspension cells correlates with an increase in cell size. *Plant Mol. Biol.* **52**, 387-400.

Rutherford, S. and Moore, I. (2002). The *Arabidopsis* Rab GTPase family: another enigma variation. *Curr. Opin. Plant Biol.* **5**, 518-528.

Scheffzek, K., Ahmadian, M. R. and Wittinghofer, A. (1998). GTPase activating proteins: helping hands to complement and active site. *Trends Biochem. Sci.* **23**, 257-262.

Singer-Kruger, B., Stenmark, H., Dusterhoft, A., Philippsen, P., Yoo, J., Gallwitz, D. and Zerial, M. (1994). Role of three rab5-like GTPases, Ypt51p, Ypt52p, and Ypt53p, in the endocytic and vacuolar protein sorting pathways of yeast. *J. Cell Biol.* **125**, 283-298.

Sivars, U., Aivazian, D. and Pfeffer, S. R. (2003). Yip3 catalyses the dissociation of endosomal Rab-GDI complexes. *Nature* **425**, 856-859.

Sohn, E. J., Kim, E. S., Zhao, M., Kim, S. J., Kim, H., Kim, Y.-W., Lee, Y. J., Hillmer, S., Sohn, U., Jiang, L. et al. (2003). Rha1, an *Arabidopsis* Rab5 Homolog, plays a critical role in the vacuolar trafficking of soluble cargo proteins. *Plant Cell* **15**, 1057-1070.

Soldati, T., Shapiro, A. D., Svejstrup, A. B. and Pfeffer, S. R. (1994). Membrane targeting of the small GTPase Rab9 is accompanied by nucleotide exchange. *Nature* **369**, 76-78.

Stenmark, H. and Olkkonen, V. M. (2001). The Rab GTPase family. *Genome Biol.* **2**, 3001-3007.

Stenmark, H., Parton, R. G., Steele-Mortimer, O., Lutcke, A., Gruenberg, J. and Zerial, M. (1994). Inhibition of rab5 GTPase activity stimulates membrane fusion in endocytosis. *EMBO J.* **13**, 1287-1296.

Tamura, K., Shimada, T., Ono, E., Tanaka, Y., Nagatani, A., Haigashi, S., Watanabe, M., Nishimura, M. and Hara-Nishimura, I. (2003). Why green fluorescent fusion proteins have not been observed in vacuoles of higher plants. *Plant J.* **35**, 545-555.

Tse, Y. C., Mo, B., Hillmer, S., Zhao, M., Wan, S., Robinson, D. and Jiang, L. (2004). Identification of multivesicular bodies as prevacuolar compartments in Nicotiana tabacum BY-2 cells. *Plant Cell* **16**, 672-693.

Ueda, T., Yamaguchi, M., Uchimiya, H. and Nakano, A. (2001). Ara6, a plant-unique novel type Rab GTPase functions in the endocytic pathway of *Arabidopsis thaliana*. *EMBO J.* **20**, 4730-4741.

Ullrich, O., Horiuchi, H., Bucci, C. and Zerial, M. (1994). Membrane association of Rab5 mediated by GDP-dissociation inhibitor and accompanied by GDP/GTP exchange. *Nature* **368**, 157-160.

Wittinghofer, F. (1998). Ras signalling: caught in the act of the switch on. *Nature* **394**, 317-320.

Zerial, M. and McBride, H. (2001). Rab proteins as membrane organizers. *Nat. Rev. Mol. Cell Biol.* **2**, 107-119.